



Nanopowder metrology and nanoparticle size measurement - Towards the development and testing of protocols

Anne Aimable, Paul Bowen*

Powder Technology Laboratory (LTP), Materials Institute, Swiss Federal Institute of Technology, Ecole Polytechnique Fédérale de Lausanne (EPFL), 1015 Lausanne, Switzerland

Received 9 February 2010; received in revised form 17 August 2010; accepted 23 August 2010

Abstract

There are many methods and instruments available for powder characterization and they are more or less well suited to powders in different size ranges. This report presents in more detail the relatively recent Centrifugal Particle Sizer (CPS) and its potential for particle size distribution measurement compared to more classical techniques (microscopy, laser diffraction, or photo correlation spectroscopy). To get reliable comparable data is of primary importance for new application developments. A series of protocols for nanosized powders - nanopowder metrology - was produced within the framework of a COST Action - COST 539 "Electroceramics from Nanopowders Produced by Non-conventional Methods". The protocols have been tested using well-characterized commercial products, and for a series of powders produced in the COST Action 539. The results show that results between methods and or laboratories are often very good but some show significant deviations illustrating the need for a systematic approach and how the protocols can help us develop a Nanometrology for new functional powders.

Keywords: *particle size measurement, nanoparticles, nanometrology*

I. Introduction

Nanoparticles have a huge potential for new applications and scientific discovery but knowledge of the life-cycle risks of nanomaterials for the environment, health and safety have to be assessed for success. An important barrier that hinders both application and health and safety issues are reliable large scale production and in particular accurate assessment of the powder characteristics (size, shape, state of agglomeration and surface chemistry). The importance of the assessment of particles size for many applications in the nanometre regime is of great interest but not always quick and easy and when the size distribution is important and not just a comparative median needed then the task is even less straightforward. For the production of ceramics from nanosized powders the particle size distribution (PSD) and state of agglomeration are essential characteristics. Agglomeration even when just a few % of the total distribution can have a huge influence on particle packing,

sintering and resulting microstructure, grain size and properties [1–3].

There are many methods and many instruments available for particle size measurement and they are more or less well suited to powders in different size ranges and size dispersions [4,5]. For nanosized powders methods for particle size measurement from 2 nm to 100 nm have more recently been investigated and assessed [6–10]. Several different techniques were evaluated such as photocentrifuge, photon correlation spectroscopy (PCS), an X-ray disc centrifuge (XDC), analytical ultracentrifuge (AU), laser diffraction (LD) and transmission electron microscopy (TEM) image analysis [6,7,9]. These methods were used to characterise the PSD of several inorganic powders (γ - Al_2O_3 , Fe_xO_y , ZnS, SiO_2). The different powders covered the size range from 2 nm to around 100 nm. The state of agglomeration and how different treatments such as, milling and surface modification affect the state of agglomeration for an "as-received" and attrition milled gamma alumina, both as a function of milling time and bead size [3,8]. The results illustrated the importance and

* Corresponding author: tel: +41 21 693 4907
fax: +41 21 693 3089, e-mail: paul.bowen@epfl.ch

usefulness of agglomeration factors and rigorous evaluation of agglomerates rather than evaluation of primary particle sizes from simple TEM observations. For the sedimentation based methods results were presented after consideration of the hydrodynamic density and the light scattering corrections used for the optical based methods. For spherical silica particles accuracies on the median size better than $\pm 20\%$ was shown to be difficult without an accurate hydrodynamic density [8]. However reliability between methods for nanosized powders narrow size distributions were shown to be around 5% for D_{v10} , D_{v50} and D_{v90} diameters. The effects on the colloidal stability of different dispersion conditions for the nanosized silicas were also investigated and showed the importance of using well characterised powders to correctly interpret nanoparticle behaviour [11]. To get reliable comparable data between different methods and different users not only do the theoretical limitations of the particular characterisation method need to be taken into account [12–19] but detailed and clear protocols for the measurement technique are essential and is the main subject of this paper.

Golden rule No. 3 in powder characterisation is to always use complimentary techniques to characterise a powder (Golden Rules No. 1 and 2 are related to sampling [4]). An easy and reliable approach to quantify the state of agglomeration of a powder is to take the ratio between the median volume diameter (d_{v50}) measured by XDC or PCS to that calculated from the specific surface area [6,7]. Although the measurement of specific surface area by nitrogen adsorption is a standard technique, for high surface area nanosized powders certain precautions and protocols have to be strictly followed. Other techniques of particular interest for the characterisation of nanosized powders are X-ray powder diffraction (phase and crystallite size from line broadening), electron microscopy for image analysis, where sample preparation before imaging is often poorly carried out leading to misleading conclusions from images. When powders have to be dispersed for forming of ceramic pieces (slip casting, filter pressing or granulation [20,21]) the surface charge and zeta potential are key factors that need to be correctly measured. Another important characteristic is density and porosity which can be characterised by helium pycnometry and full nitrogen adsorption desorption isotherms. All of these methods need a standardised protocol for nanopowders as large amounts of adsorbed water on the high surface areas can often lead to erroneous measurements, conclusions and much wasted effort in ensuing ceramic forming and sintering. Thermogravimetric analysis is a key measurement in this context too as it is very sensitive to adsorbed water and surface hydroxylation characterisation.

We have produced a series of such protocols for nanosized powders - nanopowder metrology - within the framework of a COST Action - COST 539 “Elec-

troceramics from Nanopowders Produced by Non-conventional Methods” The methodologies were developed and detailed experimental and data treatment protocols for nanoparticle size measurement and characterisation have been documented. The protocols have been tested using nanosized silica, alumina, and barium titanate from commercial sources. They have also been used for a series of powders produced in the COST Action 539 (TiO_2 , BaTiO_3 , hydroxyapatite $\text{Ca}_{10}(\text{PO}_4)_6(\text{OH})_2$, and LaNiO_3). The results show that results between methods and or laboratories are often very good but some show significant deviations illustrating the need for a systematic approach and how the protocols can help us develop a Nanometrology for new functional powders.

II. Materials and methods

2.1 Classical characterization methods in Powder technology: a brief overview

Nanomaterials and nanotechnology attract an extraordinary amount of interest. However the potentials and risks of such innovative products have to be thoroughly evaluated before being proposed to consumers as commercial products.

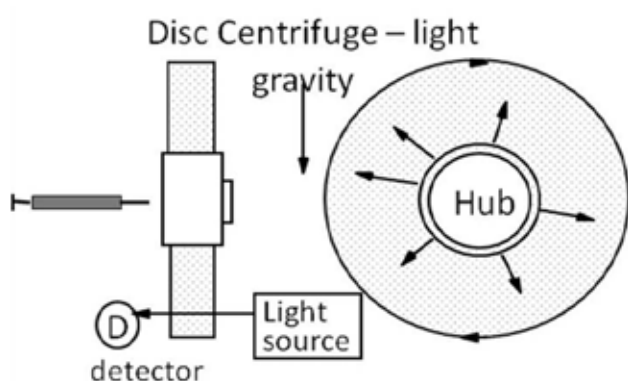
11 protocols have been written, for the complementary techniques used for the characterization of nanopowders (see Table 1), these can be downloaded from the web [22]. Most of the following methods have been described in detail elsewhere [4–6,23], except for the relatively recent Centrifugal Particle Sizer (CPS) which is described in detail below and evaluated with respect to other PSD instruments in the following section.

2.2 Description of line-start disc Centrifugal Particle Sizer: CPS

The CPS Disc Centrifuge separates particles by size using centrifugal sedimentation in a liquid medium by using the “line-start method” [4] by injecting a particle suspension onto the meniscus at the centre of the disc (Fig. 1). This has the advantage over homogeneous suspension instruments [6] in that it facilitates the light scattering correction needed for particle smaller than the wavelength of the light used to detect the sedimenting particles [24]. The sedimentation in the disc is stabilized by a slight density gradient within the liquid produced using sugar solutions. The particles sediment within an optically clear and rotating disc (maximum speed: 24000 rpm, 29000 G). The particles are measured by light absorption: when particles approach the outside edge of the rotating disc, they scatter a portion of a light beam that passes through the disc. The change in light intensity is continuously recorded, and converted by the operating software into a particle size distribution using Stokes law and assuming spherical particles. Knowledge of the refractive indices and densities of both particle and liquid are needed. The measurable size ranges from 5 nm to 40 μm . Dilute suspensions,

Table 1. Overview of the classical characterization methods

Measurement	Method	Acronym	Equipment supplier
Microscopy	Scanning Electron Microscopy	SEM	Philips XL 30 FEG
	Transmission Electron microscopy	TEM	Philips CM 200
Particle size distribution (PSD)	X-Ray Disc Centrifuge	XDC	Brookhaven
	Centrifugal Particle Sizer (light absorption/scattering)	CPS	CPS Instruments
	Laser diffraction	LD	Malvern
	Dynamic light scattering	PCS	Brookhaven
Specific surface area	Nitrogen adsorption, BET method	SSA	Micromeritics
Pore size distribution-volume, specific surface area	Nitrogen adsorption, BET, Langmuir	ASAP	Micromeritics
Density	He pycnometry	pycno	Micromeritics
Zeta potential	Phase Analysis Light Scattering	Zeta PALS	Brookhaven
	Electroacoustics	Acousto	Agilent Technologies
Phase identification, crystallite size	Powder X-Ray Diffraction	XRD	Philips X'Pert diffractometer
Temperature behaviour	Thermogravimetry	TGA	Mettler

**Figure 1. Schematic representation of the Centrifugal Particle Sizer CPS (particle detection by light absorption/scattering)**

on the order of 0.01–1.0 wt.%, are prepared, using suitable wetting and/or dispersing agents. An ultrasonic treatment is normally used in suspension preparation to break up loosely-held agglomerates. Only 100 μL of suspension are required to carry out the measurements another advantage over cuvet photocentrifuges and X-ray detection systems where significantly more powder

Table 2. Characteristics of the powders used or the measurements.

Reference powders	Density [g/cm^3]	Refractive index	Absorption
$\gamma\text{-Al}_2\text{O}_3$ Nanotek	3.60	1.77	0.01
SiO_2 Klebosol 150H	2.2	1.49	0.01
SiO_2 Klebosol 1508	2.2	1.49	0.01
BaTiO_3 ORG NBT36	5.8	2.4	0.01

is needed. The use of a variable disc speed also allows very high dynamic range of 1000 - this is very useful for powders with a very broad PSD.

2.3 Internal “reference powders”

We have produced some detailed protocols for nano-sized powders - nanopowder metrology, by using some “Internal reference powders” from commercial sources: nanosized silica (SiO_2 Klebosol 150H and Klebosol 1508, A-Z Chemicals), alumina ($\gamma\text{-Al}_2\text{O}_3$ Nanotek, Nanophase Technologies Corporation), and barium titanate (BaTiO_3 ORG NBT36 - TechPowder SA). These powders have been previously studied, which led to numerous quantitative data comparison between various techniques [6–8,11,25]. The powders cover the 20–200 nm range, typical of most current ceramic powders (Fig. 2). The PSD measurements have been repeated several times (4–6) on the same sample, and for different suspension preparations, to evaluate the reproducibility of the PSD measurements and suspension preparation.

An overview of the results obtained with different techniques on these reference powders is given in Table 3. In general the laser diffraction gives higher values due to the low sensitivity of the laser beam to sub 100 nm particles [6]. The other techniques XDC, PCS and CPS giving consistent but not exactly the same results - to ascertain which method is giving the most accurate results - image analysis is necessary and this is carried out for a series of test powders in the protocol validation later in section 4 of this article.

With a high quality of powder, such as the BaTiO_3 (Fig. 2d), a good sample preparation and the application

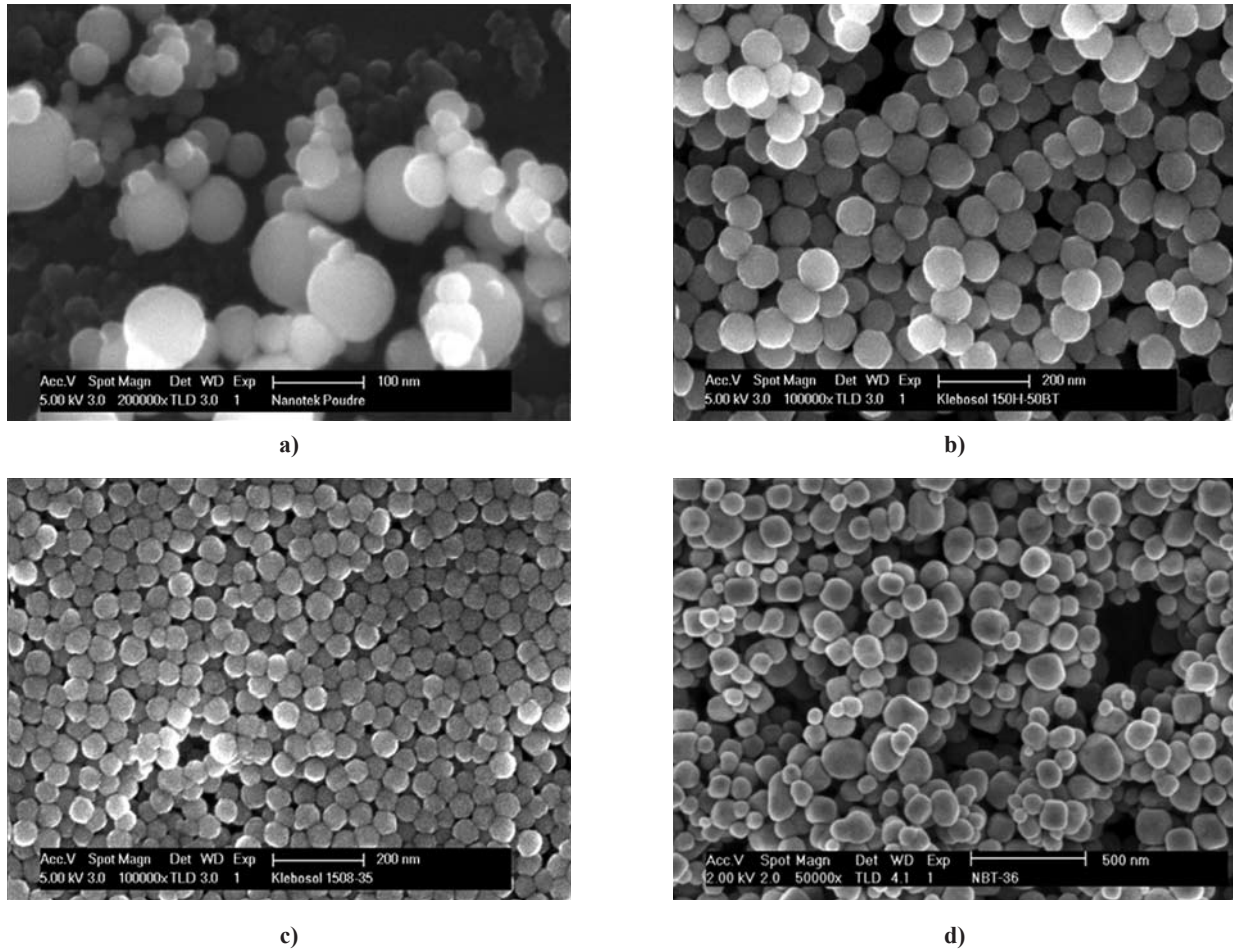


Figure 2. SEM pictures of: a) $\gamma\text{-Al}_2\text{O}_3$ Nanotek, b) SiO_2 Klebosol 150H, c) SiO_2 Klebosol 1508, d) BaTiO_3 ORG NBT36 powders

Table 3. Overview of internal reference powders characteristics

Reference powders	LD Dv_{50} [μm]	XDC Dv_{50} [μm]	PCS Dv_{50} [μm]	CPS Dv_{50} [μm]	Zeta potential at pH=6 [mV]	SSA [m^2/g]	D_{BET} [μm]
$\gamma\text{-Al}_2\text{O}_3$ Nanotek	0.210	0.061	0.055	0.099	13.8±1.9	39.7±0.3	0.044
SiO_2 Klebosol 150H	0.060	0.053	0.082	0.083	-9.2±1.8	49.0±0.4	0.056
SiO_2 Klebosol 1508	0.090	0.039	0.056	0.056	-9.7±3.2	77.8±0.2	0.035
BaTiO_3 ORG NBT36	0.190	0.164	0.130	0.162	-5.6±1.4	10.8±0.1	0.096

Table 4. CPS characterisation on BaTiO_3 reference powder - very good reproducibility, low standard deviation of the measurement (*Polydispersity index = Weight mean/Number mean*)

BaTiO_3 ORG NBT36 concentration	D_{v10} [μm]	D_{v50} [μm]	D_{v90} [μm]	D_{v99} [μm]	Polydispersity index
1.0 wt.%	0.105	0.162	0.217	0.266	1.619
12.5 wt.%	0.110	0.166	0.227	0.284	1.452
2.5 wt.%	0.107	0.164	0.220	0.270	1.422
1.0 wt.%	0.105	0.162	0.217	0.266	1.560
0.5 wt.%	0.103	0.162	0.216	0.268	1.839
0.5 wt.%	0.106	0.163	0.217	0.270	1.409
Mean size [μm]	0.106	0.163	0.219	0.271	1.550
Standard deviation [%]	2.1	1.0	1.9	2.4	10.6

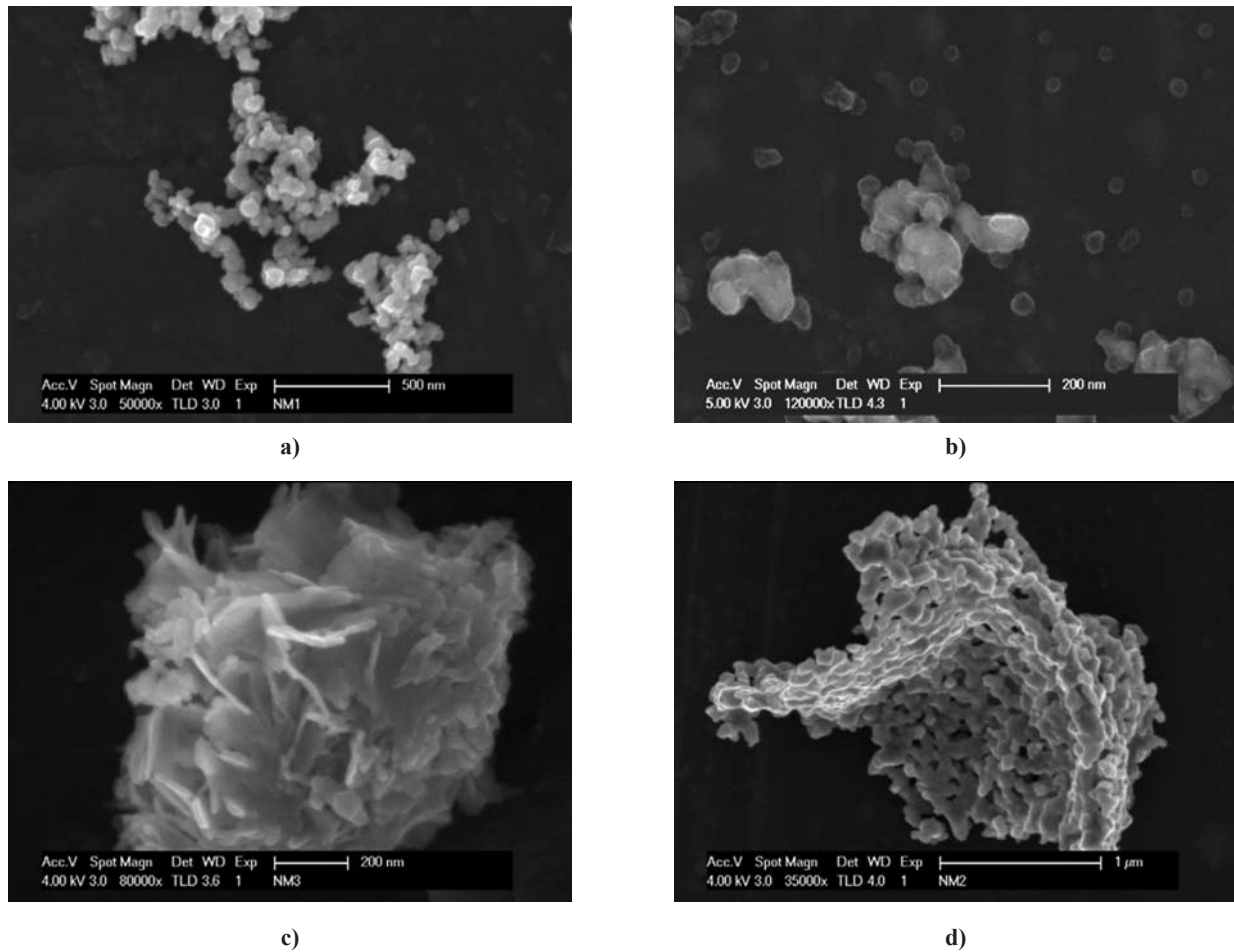


Figure 3. SEM pictures of the powders produced in the COST Action: a) titanium dioxide (TiO_2), b) barium titanate (BaTiO_3) - attrition milled, c) hydroxyapatite ($\text{Ca}_{10}(\text{PO}_4)_6(\text{OH})_2$) and d) lanthanum nickel oxide (LaNiO_3)

Table 5. CPS characterization of $\gamma\text{-Al}_2\text{O}_3$ standard powder - showing reasonable reproducibility

$\gamma\text{-Al}_2\text{O}_3$ Nanotek concentration	D_{v10} [μm]	D_{v50} [μm]	D_{v90} [μm]	D_{v99} [μm]	Polydispersity index
0.1 wt. %	0.056	0.107	0.173	0.321	1.990
0.25 wt. %	0.045	0.099	0.165	0.296	2.483
0.5 wt. %	0.044	0.097	0.166	0.295	2.241
0.5 wt. %	0.034	0.093	0.162	0.289	2.919
Mean size [μm]	0.045	0.099	0.166	0.300	2.408
Standard deviation [%]	19.9	5.9	2.8	4.7	16.4

of a well-defined protocol, very reproducible results can be achieved, with a very small standard deviation (Table 4, CPS on BaTiO_3) even with significant variations in the aliquot concentration. Comparable reproducible results were obtained from the different instruments cited in Table 3 for this high quality on BaTiO_3 powder [26,27].

III. Comparison between methods and laboratories in the COST Action

To In the COST Action Elena 539, the powder characteristics needed to be measured correctly as they touch upon three extremely important aspects: i) pow-

der synthesis, ii) production and properties of electroceramics, iii) health and safety during handling and application lifetime. Nanoparticle characterisation protocols allow synthesis routes to be evaluated and optimized, for forming and sintering of optimized powders leading to the highest quality electroceramics with nanosized microstructures and new exciting properties. The protocols also help evaluate the health and safety aspects as the powders are well defined characterized products.

The protocols have been tested for a series of powders produced in the COST Action 539 (TiO_2 , BaTiO_3 ,

hydroxyapatite $\text{Ca}_{10}(\text{PO}_4)_6(\text{OH})_2$, and LaNiO_3) shown in Fig. 3. The collected PSD data are given in Tables 6-9, and show that results between methods and or laboratories are often very good but some show significant deviations (200%), particularly for particle size measurement using different instruments. The reasons for the deviations were often associated with the experimental protocols as well as the instrumental limitations. Examples were the use of different temperatures to degas powders for SSA measurements leading to a 30% difference in values (Table 8) and the use of incorrect refractive indices for powders where the fine tail of powders were overestimated by a factor of 3 (Table 9). In this particular case the powder was very dark in colour and had a significantly higher light adsorption ($i = 1.0$) than users usually use for simply opaque powders ($i = 0.1$). The use of incorrect refractive indices usually arises when new, unknown or composite materials, often coloured or non-transparent, are being characterised. When this is the case users need to make either an educated guess by finding a compound with known op-

tical properties of a similar chemical composition or to use a “composite” refractive index normalised on the volume fraction of each component (of known or estimated refractive indices). These results illustrate the need for a systematic approach and the protocols can help us develop a Nanometrology for these new functional powders.

IV. Validation of these protocols with high quality powders

4.1 With commercial powders

Two Gold Colloids from BBInternational with nominal sizes of 20 nm and 50 nm were used for testing our protocols on commercial powders. These are commercial suspension of gold nanoparticles in an aqueous medium, with a very low dispersion in sizes. The refractive index of 0.47 was used, absorption of 1.0 and refractive index of water 1.33. For CPS measurements the disc rotation was set at a high level of 20000 rpm to attain such small sizes in a reasonable time (20 to 60 minutes). We used a density of 16 g/cm^3 , a bit lower than the theoretical one

Table 6. Characterization of TiO_2 produced in the COST Action

	Method	D_{v10} [μm]	D_{v50} [μm]	D_{v90} [μm]
TiO_2	LD (Malvern)	0.10	0.28	0.78
	CPS	0.06	0.11	0.21
$SSA = 65.6 \text{ m}^2/\text{g} - d_{BET} = 47.4 \text{ nm}$ $Fag = 2.3$ - Well dispersed, low agglomeration factor				

Table 7. Characterization of BaTiO_3 produced in the COST Action

	Method	D_{v10} [μm]	D_{v50} [μm]	D_{v90} [μm]
BaTiO_3 -attrition milled	LD (Malvern)	0.32	0.69	1.52
	CPS	0.14	0.37	0.73
$SSA = 19.9 \text{ m}^2/\text{g} - d_{BET} = 50.3 \text{ nm}$ $Fag = 13.7$ - Heavily agglomerated				

Table 8. Characterization of hydroxyapatite produced in the COST Action

	Method	D_{v10} [μm]	D_{v50} [μm]	D_{v90} [μm]
$\text{Ca}_{10}(\text{PO}_4)_6(\text{OH})_2$ hydroxyapatite	LD (Malvern)	2.03	5.52	13.27
		$SSA = 79.6 \text{ m}^2/\text{g} - d_{BET} = 23.9 \text{ nm}$ Nominal $SSA = 120 \text{ m}^2/\text{g}$ - degassing of the powder not done at same temperature $Fag = 230$ -Heavily agglomerated, shape-plate like, difficult to characterize		

Table 9. Characterization of LaNiO_3 produced in the COST Action

	Method	D_{v10} [μm]	D_{v50} [μm]	D_{v90} [μm]
LaNiO_3	LD (Malvern) <i>abs 0.1 (incorrect)</i>	0.07	1.12	6.38
	LD <i>abs 1.0 (correct)</i>	0.22	0.96	3.07
	CPS	0.19	0.33	0.70
	XDC	0.47	0.73	1.73
$SSA = 10.1 \text{ m}^2/\text{g} - d_{BET} = 81.5 \text{ nm}$ $Fag = 11.8$ - Heavily agglomerated, shape irregular, difficult to characterize				

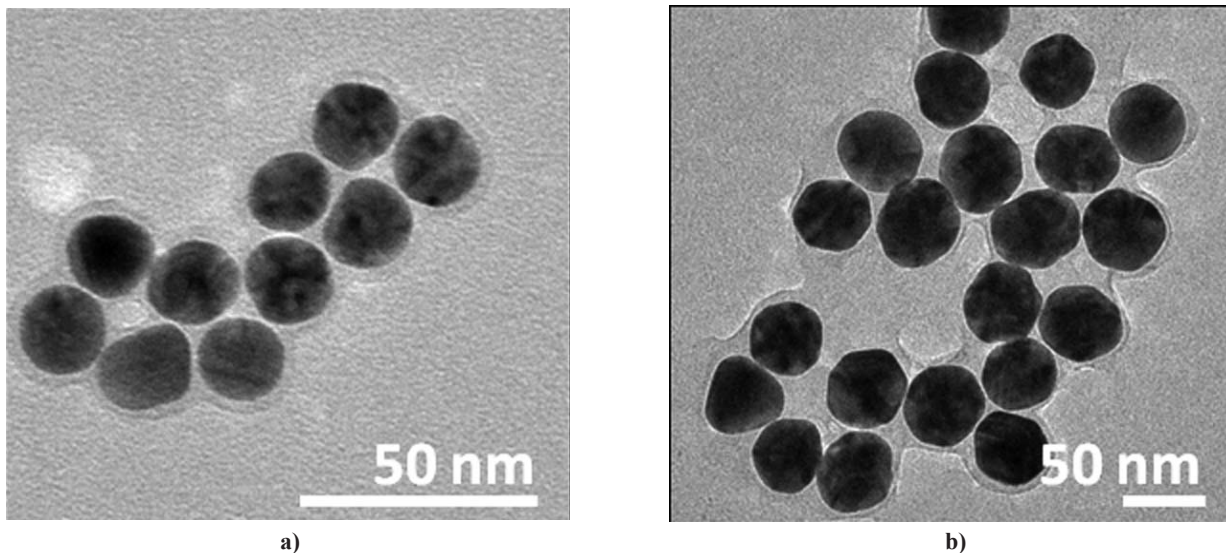


Figure 4. TEM pictures of Gold Colloid particles: a) 20 nm and b) 50 nm

Table 10. Comparison of sizes measured by TEM, CPS and PCS, on commercial gold nanoparticles

	Method	TEM	CPS	PCS
Gold Colloid 20 nm	$D_{TEM} - D_{v50}$ [nm]	18.4	17.3	15.6
	Standard deviation [nm]	1.9	0.1	0.3
Gold Colloid 50 nm	$D_{TEM} - D_{v50}$ [nm]	47.7	48.1	50.1
	Standard deviation [nm]	2.3	0.3	1.2

of 19.4 g/cm³, corresponding to an adsorbed layer of water or surfactant at the surface of 1.7 nm, which is very realistic. A halo of 1–2 nm is observed around the particles on all TEM pictures (Fig. 4), which can probably come from the drying of these adsorbed species and is consistent with other studies on iron oxide nanoparticles [8].

We compared 3 methods PSD measurement: TEM, CPS and PCS (Table 10). The PSD measurements for CPS and PCS have been repeated several times (4–6) on the same sample, and for different suspension preparations, and on 100 particles for TEM.

There is a very good agreement in the D_{v50} measured by TEM, PCS and CPS for particles around 50 nm,

whereas there is a larger discrepancy for the 20 nm particles. However the particle size distributions measured by these 2 methods are similar (Fig. 5) with broader distributions measured by PCS in both samples. TEM suggests the PCS to be better whereas the CPS may be suffering from particle-particle interactions inducing cooperative sedimentation at these high g forces leading to the very sharp distributions [10].

As a second example, PSDs were measured by two methods - CPS and PCS - on nanoparticles reference materials provided by the IRMM (Institute for Reference Materials and Measurements). The samples provided were 10 mL pre-scored ampoules containing 9 mL of

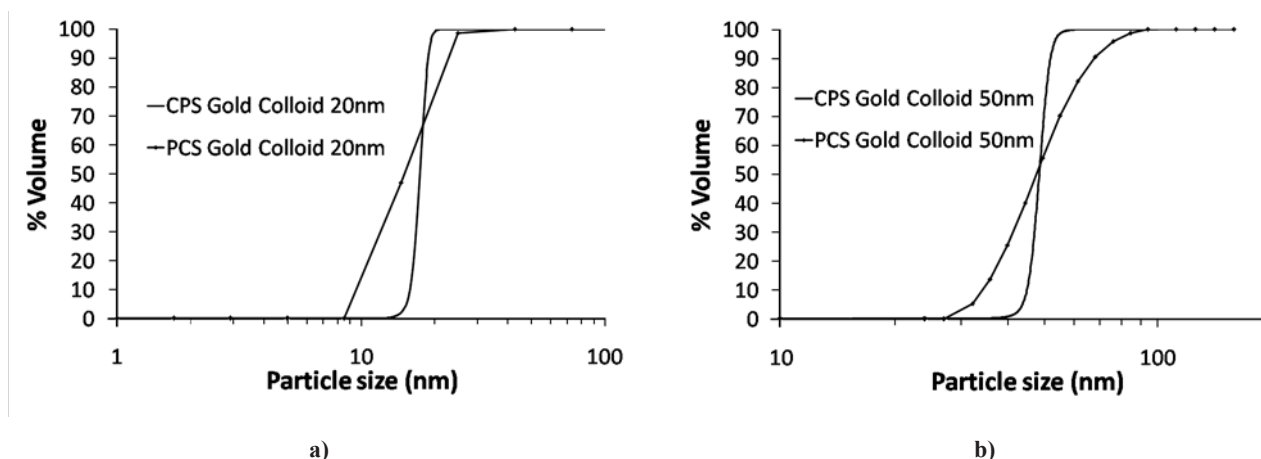


Figure 5. Particle size distributions of Gold Colloid particles - 20 nm (a) and 50 nm (b) - measured by CPS and PCS

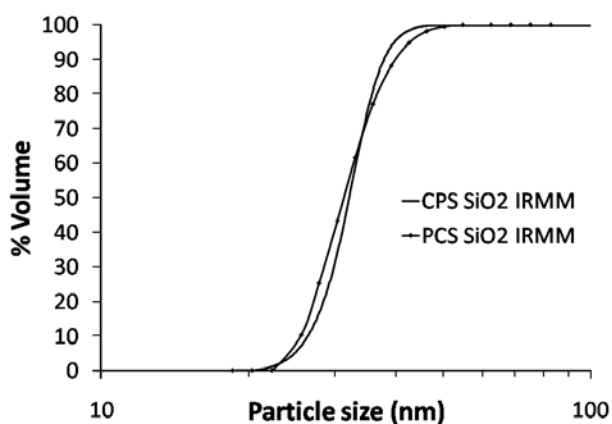


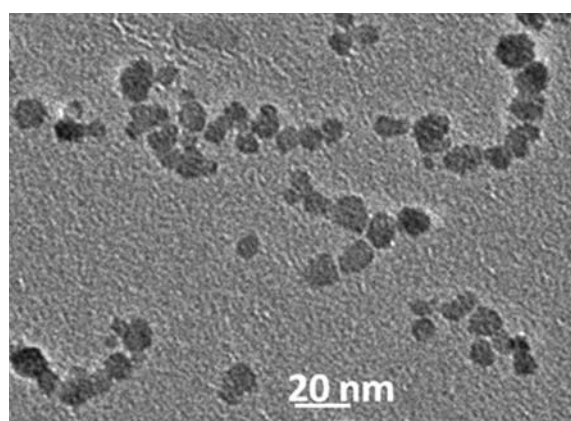
Figure 6. Particle size distributions of silica suspensions provided by IRMM for standardization, measured by CPS and PCS

Table 11. Comparison of sizes measured by CPS and PCS on SPIONs on three different separate samples

	D_{v10}	D_{v50}	D_{v90}
PCS [nm]	9.9	12.4	19.6
Standard deviation [nm]	0.4	0.7	1.9
CPS [nm]	7.5	10.1	13.8
Standard deviation [nm]	0.1	0.1	0.1

Table 12. Comparison of sizes measured by CPS and PCS on ZnO nanoparticles

	D_{v10}	D_{v50}	D_{v90}
PCS [nm]	52.7	66.7	119.9
Standard deviation [nm]	2.0	2.7	4.3
CPS [nm]	43.1	63.9	85.0
Standard deviation [nm]	1.1	2.4	3.2



a)

suspended silica nanoparticles (SiO_2). The suspending medium is water-based and contains a small amount of NaOH as stabilizing agent ($\text{pH} = 8.6$), with a nominal relative particle mass fraction of 0.75%.

Due to the quasi-monodispersity of the samples, CPS and PCS measurements can be almost superimposed (Fig. 6). Results gave an excellent reproducibility between the different samples and batches ($D_{v50} = 31.9 \pm 0.1$). These results and the results with the Gold particles show that both the protocols and instruments PCS and CPS are well suited for the sub 100 nm range. In the next section we will use these methods to characterize powders synthesized in the laboratory.

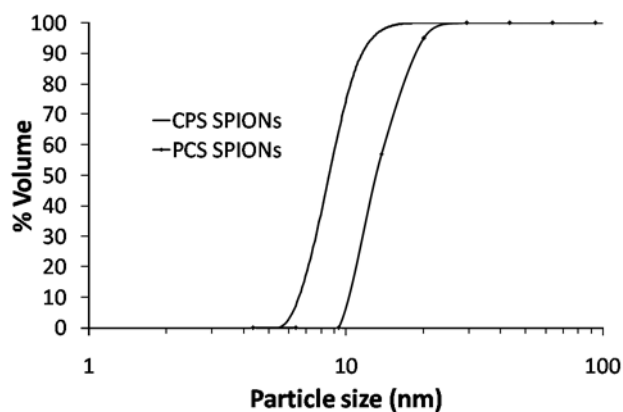
4.2 With powders produced in the laboratory

Our protocols were finally tested on iron oxide and zinc oxide nanoparticles produced in our laboratory. Very good results were obtained due to the high quality of powders and suitability of the protocols.

Superparamagnetic iron oxide nanoparticles (SPIO-Ns) were prepared by alkaline co-precipitation of ferric and ferrous chlorides in aqueous solution, followed by a reduction step by iron nitrate with nitric acid under reflux. The obtained brown suspension was dialyzed against 0.01 M nitric acid for 2 days (further details can be found elsewhere [28]).

For PCS measurement, the suspension (1 mg/mL in HNO_3 0.01 M) was diluted 10 times with ultra-pure water. The refractive index of iron oxide 2.4 was used, absorption of 0.1 and refractive index of water 1.33. For CPS measurements the disc rotation was set at the maximum level of 24000 rpm to attain such small sizes in a reasonable time (about 2 hours). We used the suspension as synthesized (1 mg/mL), and the density of 4.9 g/cm^3 determined by other methods [28].

The particle size distributions measured by CPS and PCS are very close, as shown on Fig. 7b and Table 11. PCS gives a higher diameter because this analysis measures the hydrodynamic diameter. Thus even though the standard size is far from the range of the calibration measurement (PVC particles: 377 nm), CPS remains a very reliable technique for well suspended nanoparticles.



b)

Figure 7. (a) TEM picture of SPIONs, (b) Particle size distributions measured by CPS and PCS on SPIONs suspension

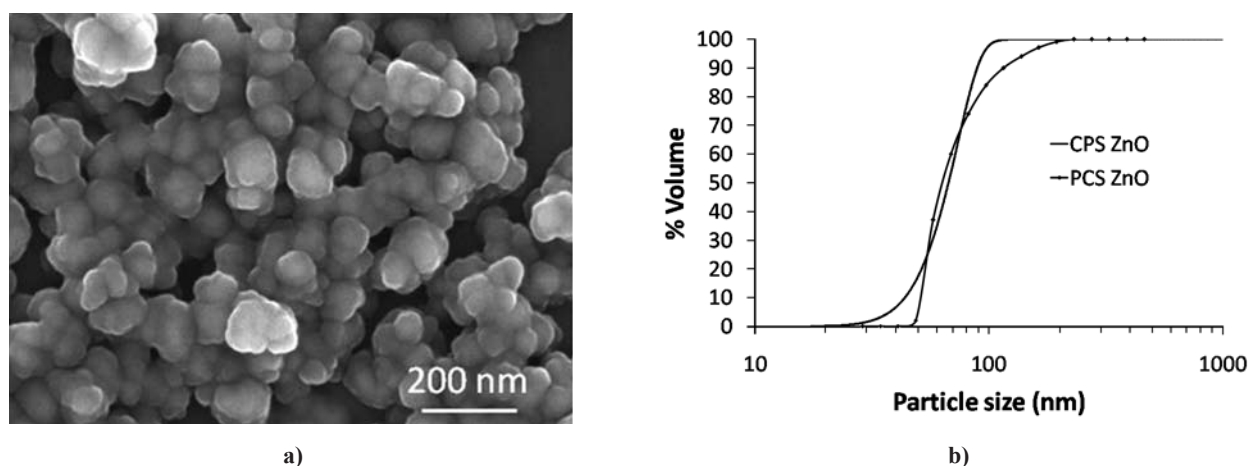
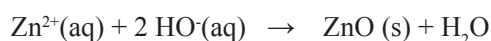


Figure 8. (a) TEM picture of precipitated ZnO, (b) Particle size distributions measured by CPS and PCS on ZnO suspension (1.0 wt.% in PAA solution at 0.1 wt.% - $R = 1.5$)

The precipitation of ZnO results from the mixing of zinc nitrate and sodium hydroxide aqueous solutions:



The Zn^{2+} reaction solution at 0.10 M was prepared by dissolving $\text{Zn}(\text{NO}_3)_2 \cdot 6\text{H}_2\text{O}$ in ultra pure water. The NaOH reaction solution at 0.11 M was prepared by diluting a titrated solution NaOH 1 M in ultra pure water. Poly(acrylic acid) (PAA M_w 2000) at 0.05 wt.% was added in the NaOH reaction solution for a better control of the precipitated powder [29]. After reaction, the suspended powder was washed 4 times with ultra pure water, before being filtered and dried for 24 hours at 70°C.

For CPS measurement, a suspension was prepared by dispersing 0.1 g of powder in 40 g of solution of polyacrylic acid (PAA) $M_w \sim 2000\text{g/mol}$, 0.1 wt.%, pH = 10 (filtered at 0.2 μm), and treated with an ultrasonic horn for 15 minutes, cooled in an ice bath. The disc rotation was set at 15000 rpm. We used the theoretical density of zinc oxide 5.6 g/cm^3 , the refractive index 2.1, and 0.1 for the absorption. For PCS, same values were used, but the suspension was diluted 100 times in ultra-pure water.

The particle size distributions measured by CPS and PCS can almost superimpose: $D_{v50}(\text{CPS}) = 63.9 \text{ nm}$, and $D_{v50}(\text{PCS}) = 66.7 \text{ nm}$ (Fig. 8b and Table 12).

These various high quality “home-made” and commercial powders could be used as “reference materials” to validate to correct functioning of instruments and laboratory protocols. They have already been used successfully in two external laboratories to evaluate different instruments which were giving very different results allowing us to identify operating problems and confirm the reliability of our protocols.

V. Conclusions

We have produced a series of protocols for the development of nanometrology working practices with instruments and methods used currently in our laboratory.

We evaluated a new acquisition the Centrifugal Particle Sizer (CPS) which is a line-start instrument using light for particle detection.

It was shown to be a reliable instrument working in a wider size range than Dynamic light scattering (PCS) and in some cases more reliable as it is less sensitive to anomalies, such as multiple scattering or dust. It is more adapted to nanometric sizes than laser diffraction which tended to oversize the particle size. The analysis using the CPS is faster than the X-Ray Disc Centrifuge (XDC), and requires smaller amount of material (mg compared to g). In conclusion it is very reliable and practical equipment for measuring particle size distributions of nanometric to micronic particles.

The use of measurement protocols proved to be necessary for reliability and reproducibility of measurements. They constitute a strong basis and are necessary for comparison of results obtained on different instruments or from different users. These nanoparticle characterisation protocols were tested within the framework of the COST Action 539 and allowed synthesis routes to be better evaluated and optimised. As a result the forming and sintering of optimised powders should lead to the highest quality ceramics with nanosized microstructures and possibly new properties. The protocols can also help evaluate the health and safety aspects, as the test powders are well defined fully characterised products.

Acknowledgements: The authors would like to acknowledge C. Morais and E. Gonzalez for data collection and the COST Action 539 and the Swiss Costs office for support and funding.

References

1. F-S. Shiau, T-T. Fang, T-H Leu, “Effects of milling and particle size distribution on the sintering behavior and the evolution of the microstructure in sintering powder compacts”, *Mater. Chem. Phys.*, **57** (1998) 33–40.

2. P. Bowen, C. Carry, “From powders to sintered pieces: forming, transformations and sintering of nanostructured ceramic oxides”, *Powder Technol.*, **128** (2002) 248–255.
3. P. Bowen, C. Carry, D. Luxembourg, H. Hofmann, “Colloidal processing and sintering of nanosized transition aluminas”, *Powder Technol.*, **157** (2005) 100–107.
4. T. Allen, *Particle Size Measurement*, Fifth Edition, Chapman and Hall, New York, 1997.
5. B.H. Kaye, *Characterization of Powders and Aerosols*, WILEY-VCH Verlag GmbH, 1999.
6. P. Bowen, “Particle size distribution measurement from millimeters to nanometers and from rods to platelets”, *J. Disper. Sci. Technol.*, **23** [5] (2002) 631–662.
7. M. Staiger, P. Bowen, J. Ketterer, J. Bohonek, “Particle size distribution measurement and assessment of agglomeration of commercial nanosized ceramic particles”, *J. Disper. Sci. Technol.*, **23** [5] (2002) 619–630.
8. P. Bowen, M. Chastellain, F. Juillerat, M. Coignac, H. Hofmann, “Inorganic particle size measurement below 100 nm - Where life gets difficult”, *Science et Technologie des Poudres 4* (Compiègne, May 4-6, 2004) Progrès Recent en Genie de Procédés, No. 91, 2004 (CD-ISBN No. 2-910239-65).
9. H. Cölfen, T. Pauck, “Determination of particle size distributions with angström resolution”, *Colloid Polym. Sci.*, **275** (1997) 175–180.
10. Y. Dieckmann, H. Cölfen, H. Hofmann, “Particle size distribution measurements of manganese-doped ZnS nanoparticles”, *Anal. Chem.*, **81** [10] (2009) 3889–3895.
11. M. Kobayashi, P. Galetto, M. Borkovec, F. Juillerat, P. Bowen, “Aggregation rates and charging behaviour of colloidal silica particles: Effect of particle size”, *Langmuir*, **21** (2005) 5761–5769.
12. B.J. Azzopardi, *Particle Size Analysis*, (pp. 108) N.G. Stanley-Wood, R.W. Lines, Royal Society of Chemistry, Cambridge, 1992.
13. M. Khalili, W.L. Roricht, S.Y.L. Lee, “An investigation to determine the precision for measuring particle size distribution by laser diffraction”, paper 111, *World Congress on Particle Technology*, Sydney 2002.
14. R. Xu, O.A. Di Guida, “Particle size and shape analysis using light scattering, coulter principle, and image analysis”, paper 41, *World Congress Particle Technology*, Sydney, 2002.
15. P. Bowen, J. Sheng, N. Jongen, “Particle size distribution measurement of anisotropic particles - cylinders and platelets - practical examples”, *Powder Technol.*, **128** (2002) 256–261.
16. N. Gabas, N. Hiquily, C. Laguérie, “Response of laser diffraction particle sizer to anisometric particles”, *Part. Part. Syst. Character.*, **2** (1994) 121–126.
17. R.N. Kelly, K.J. DiSante, E. Stranzl, J.A. Kazanjian, P. Bowen, T. Matsuyama, N. Gabas. “Graphical comparison of image analysis and laser diffraction particle, size analysis data obtained from the measurements of nonspherical particle systems”, *AAPS Pharm. Sci. Tech.*, **7** [3] (2006) 69 (E1–14).
18. J.I. Langford, A.J.C. Wilson, “Scherrer after sixty years: A survey and some new results in the determination of crystallite size”, *J. Appl. Cryst.*, **11** (1978) 102–113.
19. D. Balzar, N. Audebrand, M. Daymond, A. Fitch, A. Hewat, J.I. Langford, A. Le Bail, D. Louër, O. Masson, C.N. McCowan, N.C. Popa, P.W. Stephens, B. Toby, “Size-strain line-broadening analysis of the ceria round-robin sample”, *J. Appl. Crystallogr.*, **37** (2004) 911–924.
20. P. Bowen, R. Mulone, P. Streit, “Processing of ceramic-metal composites (cermets) $\text{Al}_2\text{O}_3\text{-TiC}_x\text{N}_{1-x}\text{-Mo}_2\text{C-Ni}$ ”, pp. 621 in *Ceramic Transactions Vol. 51*, eds. H. Hausner, G.L. Messing, S-I. Hirano, The American Ceramic Society, 1995.
21. P. Bowen, A. Mocellin, “Pressure filtration of AlN-TiO_2 slurries for the production of reaction hot-pressed $\text{Al}_2\text{O}_3/\text{TiN}$ composites”, pp. 427 in *Ceramic Transactions Vol. 51*, eds. H. Hausner, G.L. Messing, S-I. Hirano, The American Ceramic Society, 1995.
22. <http://ltp.epfl.ch/page68789.html>
23. P.A. Webb, C. Orr, *Analytical methods in fine particle technology*, Micromeritics, 1997.
24. P. Bowen, C. Herard, R. Humprey-Baker, E. Sato, “Accurate sub-micron particle size measurement of alumina and quartz powders using a cuvet photocentrifuge”, *Powder Technol.*, **81** (1994) 235–240.
25. M. Azar, P. Palmero, M. Lombardi, V. Gamier, L. Montanaro, G. Fantozzi, J. Chevalier, “Effect of initial particle packing on the sintering of nanostructured transition alumina”, *J. Eur. Ceram. Soc.*, **28** [6] (2008) 1121–1128.
26. P. Bowen, A. Testino, V. Legagneur, M. Donnet, H. Hofmann, N. Cobut, “Precipitation of nanostructured & ultrafine powders: Process intensification using the segmented flow tubular reactor - Still in search of the perfect powder?”, *Proceedings of Fifth World Congress on Particle Technology (WCPT5)*, Orlando, USA, 2006.
27. A. Aimable, N. Jongen, A. Testino, M. Donnet, J. Lemaitre, H. Hofmann, P. Bowen, “Precipitation of nanosized and nanostructured powders: process intensification using SFTR, applied to BaTiO_3 , CaCO_3 and ZnO ”, submitted to *Chem. Eng. Technol.*, 2010.
28. M. Chastellain, A. Petri, H. Hofmann, “Superparamagnetic iron oxide nanoparticles for biomedical application: a focus on PVA as a coating”, p. N11.21 in *Quantum Dots, Nanoparticles and Nanowires Vol. 789*, eds. by P. Guyot-Sionnest, H. Mattoussi, U. Woggon, Z.-L. Wang, *Materials Research Society, Pittsburgh, 2003*.
29. A. Aimable, M.T. Buscaglia, V. Buscaglia, P. Bowen, “Polymer-assisted precipitation of ZnO nanoparticles with narrow particle size distribution”, *J. Eur. Ceram. Soc.*, **30** [2] (2010), 591–598.